Proceedings of the XVIII ECSMGE 2024
GEOTECHNICAL ENGINEERING CHALLENGES
TO MEET CURRENT AND EMERGING NEEDS OF SOCIETY

ISBN 978-1-032-54816-6
DOI 10.1201/9781003431749-332

Failure in cohesive soil due to hydraulically induced fractures

Rupture d'un sol cohésif due à des fractures d'origine hydraulique

H. Machacek*, B. Odenwald
Federal Waterways Engineering and Research Institute, Karlsruhe, Germany

K.J. Witt
Bauhaus University Weimar, Weimar, Germany

**helen.machacek@baw.de*

ABSTRACT: According to Eurocode 7 the verification against hydraulic heave on the downstream side of a sheet pile wall must be fulfilled independent from the ground properties. The mechanism of hydraulic heave is based on the soil behaviour of non-cohesive soil, in which the upward directed seepage forces on the downstream side can cause liquefaction if the effective stress is reduced to zero. However, other failure mechanisms are expected in cohesive soil due to additional binding forces. Laboratory experiments have shown, that the alternative failure mechanism in cohesive soil is triggered by the formation of fractures at the foot of the sheet pile where high hydraulic gradients occur. To further investigate the mechanisms of these hydraulically induced fractures in cohesive soils, a new triaxial test has been developed, in which the pore water pressure in the centre of the specimen is increased until failure by fracturing occurs. The pore water pressure at fracture initiation, the fracturing pressure, is a measure for the soil resistance against hydraulic induced fractures. In an extensive laboratory study the influencing factors on the fracturing pressure have been determined by variation of the sampling material, the rate of the pore water pressure increase, the stress and drainage conditions. Further insight into the stress state at fracture initiation could be gained by numerical calculations. It could be concluded, that the failure by fracture differs significantly from the failure mechanisms in cohesionless soil. Therefore new concepts are required to ensure the safety against hydraulic failure.

RÉSUMÉ: Selon l'Eurocode 7, la vérification contre le soulèvement hydraulique du côté aval d'un mur de palplanches doit être réalisée indépendamment des propriétés du sol. Le mécanisme de soulèvement hydraulique est basé sur le comportement du sol non cohésif, dans lequel les forces d'infiltration dirigées vers le haut sur le côté aval peuvent provoquer une liquéfaction si la contrainte effective est réduite à zéro. Cependant, d'autres mécanismes de rupture sont attendus dans les sols cohésifs en raison de forces de liaison supplémentaires. Des expériences en laboratoire ont montré que l'autre mécanisme de rupture dans un sol cohésif est déclenché par la formation de fractures au pied de la palplanche, là où les gradients hydrauliques sont élevés. Pour étudier plus avant les mécanismes de ces fractures d'origine hydraulique dans les sols cohésifs, un nouvel essai triaxial a été mis au point, dans lequel la pression de l'eau interstitielle au centre de l'échantillon est augmentée jusqu'à ce qu'une rupture par fracturation se produise. La pression de l'eau interstitielle à l'initiation de la fracture, la pression d'initiation, est une mesure de la résistance du sol aux fractures induites par l'hydraulique. Dans le cadre d'une étude approfondie en laboratoire, les facteurs influençant la pression d'amorçage ont été déterminés par la variation du matériau d'échantillonnage, le taux d'augmentation de la pression de l'eau interstitielle, la contrainte et les conditions de drainage. Des calculs numériques permettraient de mieux comprendre l'état de contrainte au moment de l'initiation de la fracture. On peut conclure que la rupture par fracture diffère considérablement des mécanismes de rupture dans un sol sans cohésion. Par conséquent, de nouveaux concepts sont nécessaires pour garantir la sécurité contre les ruptures hydrauliques.

Keywords: Hydraulic failure; fractures; cohesive soil; laboratory study.

1 INTRODUCTION

When dimensioning sheet piles for excavations in groundwater or along canals, the verifications against hydraulic failure mechanisms are often decisive for the required embedment depth. The current standardisation according to EC7 requires among other the verification against hydraulic heave, which is to be carried out on the basis of a force equilibrium from the soil's deadweight under buoyancy and the upward flow force, almost independent from the existing ground. However, this verification concept is based on the hydraulic failure mechanism in non-cohesive soils, where the flow force can cause soil liquefaction in the downstream area. Only in highly cohesive soils is it common practice to dispense with the verification against hydraulic heave and instead to perform the verification against uplift. The actual hydraulic failure mechanisms in fine-grained soils have been little studied, which is why both verifications are not very accurate.

Laboratory tests by (Wudtke, 2014) on a wall in silt and clay conducted by undercurrent have shown that the hydraulic failure mechanism in fine-grained soils is triggered by hydraulically induced fractures at the base of the wall. Since the subsequent sequence of failure ending in the loss of the earth abutment can proceed quickly and unnoticed, the hydraulically induced fracture initiation is decisive for the design.

But currently there is neither practical experience nor sufficient theoretical basis to determine the resistance to hydraulic fracture failure in fine-grained soils. Although various fields of geotechnics and geomechanics have been dealing with the formation and propagation of hydraulically induced fractures in rock or sand for decades, no study has yet comprehensively considered a greater number of potentially relevant influencing factors on fracture formation in fine-grained subsoil (Günther, 2019). In order to formulate a design concept against hydraulically induced fractures in fine-grained soils, it is essential to investigate the main factors influencing fracture resistance of these soils experimentally.

2 EXPERIMENTAL STUDY

To fill this knowledge gap, a laboratory study was carried out in a new type of triaxial test. In this test, the failure of the cylindrical sample (height= diameter=100mm) is not caused by shearing, but by an excess pore water pressure applied in its centre. For this purpose, a cannula with a filter tip was attached to the top plate of the triaxial device, where the pore water pressure is increased until fracture occurs. As fractures initiate at flaws in the material (Jaworski et al., 1981), the samples must be as homogeneous as possible to ensure reproducible test results.

The test setup, test procedure and sample preparation are described in detail in (Günther, 2019), (Machacek, 2024) and (Machacek and Odenwald, 2023). The resistance of a sample to hydraulically induced fractures is determined by the pore water pressure at the filter tip required for the first fracture to form. This pressure is referred to as the fracturing pressure $p_{w,fr}$. At the moment of fracture initiation there is a significant pressure drop at the controller of the pore pressure at the filter tip and at simultaneously a sharp increase in the volumes flowing in and out of the sample at the top and bottom plate (in case of drained boundary conditions). This is exemplified in Figure 1 with diagrams of the pressure curves over the time for the filter tip and the end plates (left) and the corresponding volume curves over the pressure at the filter tip (right) during the hydraulic loading.

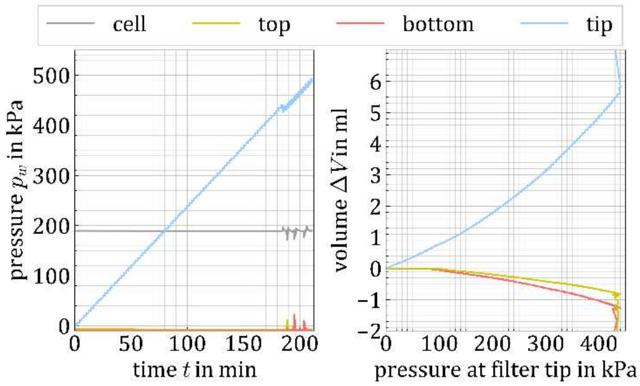

Figure 1. Typical results of the triaxial test with hydraulic loading. Left: pressure vs time for a pressure controlled loading phase with open drainage at the end plates, the pressure drop at the filter tip indicates the fracturing pressure. Right: volume change vs the pressure at the filter tip. The in- and outflowing volumes increase suddenly as the fracturing pressure is reached.

2.1 Variations

In order to investigate the soil-mechanical parameters influencing the resistance to hydraulic fractures and the fracturing pressure numerous variations with different initial and boundary conditions were carried out as part of the laboratory study.

To analyse the influence of the soil type and structure, test samples made of silt, kaolin or bentonite were loaded until fracture failure. These were either consolidated as described in (Günther, 2019) or produced by static compaction, whereby the compaction, in contrast to the consolidation, produces a soil structure with clear aggregate formation.

To vary the initial stress state, the samples were consolidated to different initial mean effective stresses p at isotropic ($\sigma_h = \sigma_v$) or anisotropic stress ratios ($K = \sigma_h/\sigma_v \neq 1$) prior to hydraulic loading. The effect of preloading by a consolidation pressure p_c was investigated by different overconsolidation ratios $OCR = p_c/p$. With regard to the hydraulic loading, variations were made between pressure and volume controlled loading with different pressure rates or volume flows. This rate of hydraulic loading must always be related to the hydraulic permeability of the sample material, so that the ratio between the flow velocity v and the permeability coefficient k is decisive.

Furthermore, tests were carried out with and without drainage at the end plates during the loading phase and the backpressure was varied during the loading phase, which influences the speed of pore water pressure propagation.

To ensure the reproducibility of the tests with hydraulic loading each variation was repeated at least two to four times under identical conditions.

2.2 Results

The fracturing pressure $p_{w,fr}$ is reproducible. Depending on the test variant, the coefficient of variation is a maximum of 17.2% and, with a mean value of 5.7%, is below the coefficient obtained in undrained triaxial shear tests carried out on the same samples.

The fracture pattern and the expansion of the fracture surfaces can be visualised by injecting potassium permanganate into the cannula after removing the sample from the triaxial cell. However, no regularity with regard to the fracture formation can be determined. Yet Figure 2 shows some fractured samples to give a better idea of the failure patterns. Fracture propagation is very complex an depends on numerous factors, which is why the following investigation focusses exclusively on factors influencing the fracturing pressure $p_{w,fr}$.

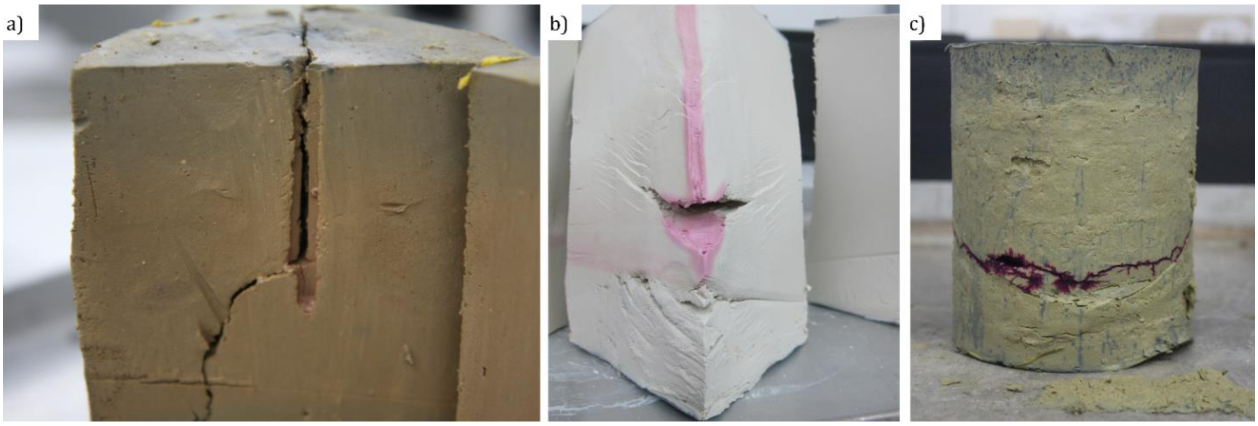

Figure 2. Examples of the fracture patterns observed by injecting potassium permanganate (purple) after removing the sample from the cell. a) A vertical fracture in a silt sample. b) Slightly horizontal fractured kaolin sample. c) A diagonal fracture through a bentonite sample.

The variations in the laboratory study showed that the magnitude of $p_{w,fr}$ was mainly influenced by the material, the initial stress state, the overconsolidation ratio OCR and the rate of the loading pore pressure (or the v/k-ratio). The other variations had minor influence on $p_{w,fr}$.

Regarding the sample material $p_{w,fr}$ increased with the amount of fines in the material. Hence the lowest fracturing pressures were observed in the silt samples and the highest in the bentonite samples. Only consolidated samples show reproducible results, in compacted samples the range of the fracturing pressures was comparatively large due to the larger aggregates and variation in pore size. Though under the same testing conditions the consolidated samples clearly show higher fracturing pressures than the compacted samples.

Further the fracturing pressure increases with the initial effective mean stress p and the overconsolidation ratio OCR. For the isotropic stress state there is an almost linear relationship between p and the fracturing pressure. The variation of the initial stress ratio K for normally consolidated samples ($OCR = 1$) shows that the fracturing pressure does not depend solely on the smaller principal stress σ_h, but on the stress state.

To compare the fracturing pressures resulting from tests with different OCR, $p_{w,fr}$ is normalised by p. The normalised fracturing pressure increases asymptotically and reaches a maximum value of $p_{w,fr}/p \sim 4$ at $OCR \sim 8$.

One of the most important influence factors is the pressure rate or the v/k -ratio. The higher the v/k -ratio, the higher the fracturing pressure. From the test results it can be assumed that the injected water does not infiltrate into the pores of the sample if the v/k -ratio is very high. Instead the soil around the filter tip is displaced and the expanding cavity is filled with the injected water.

A more detailed description of the quantitative results of the study would go beyond the scope of this article and therefore reference is made here to (Machacek, 2024).

3 NUMERICAL ANALYSIS

For the fracture failure by hydraulic loading from the centre of the sample, only the local stress state around the filter tip where the fracture first occurs is of interest. So far no analytical can describe the stress changes around the filter tip due to the pore pressure increase regarding all the influence factors observed in the laboratory study. Hence, to analyse the stress state which leads to the fracture failure a numerical analysis is required which considers the transient coupling between soil as a continuum and pore water.

3.1 Numerical model

An axisymmetric FE-model of the sample was created to simulate the tests in the laboratory study. Thereby only the stress state in the soil as a continuum until the first fracture occurs was regarded. It is not the intention to model the fracture initiation or propagation. For the material behaviour the Modified Camclay-Model (MCC) was chosen and the material parameters were calibrated from standard compression and triaxal tests. The dimensions, the (loading) boundary conditions and the mesh are shown Figure 3. To start from realistic stress states, not only the hydraulic loading but also the consolidation phases were simulated.

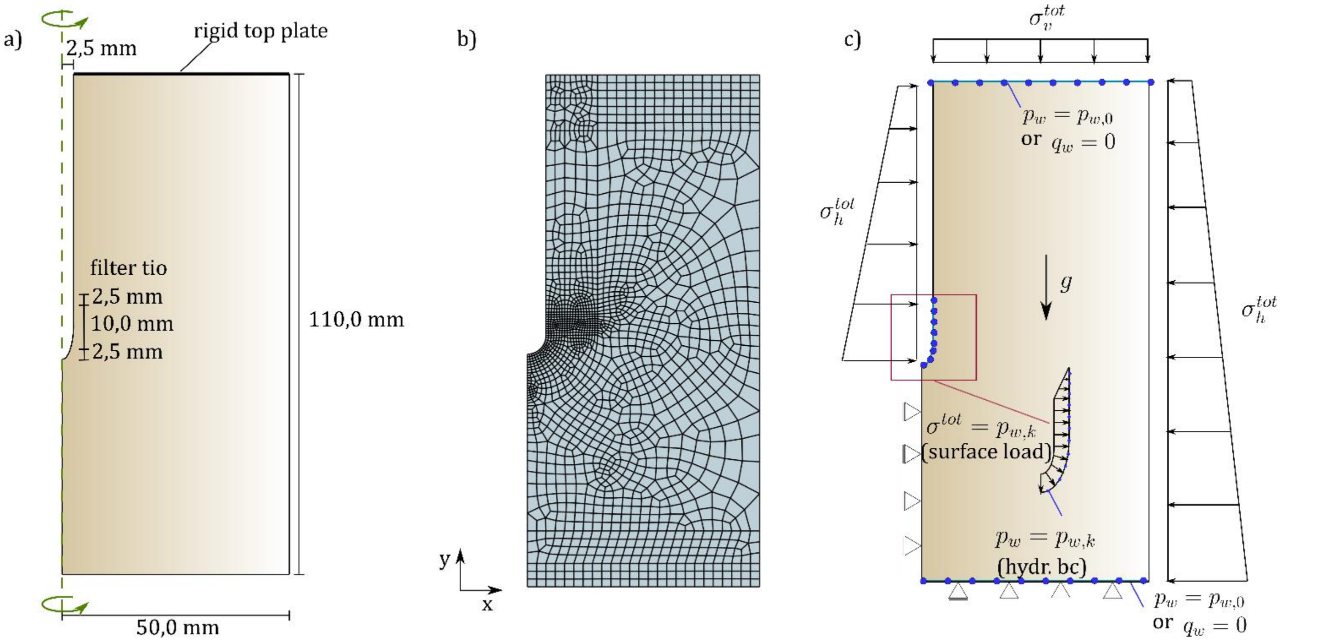

Figure 3. Axisymmetric FE-model of the triaxial test with hydraulic loading. a) Dimensions of the modelled sample. b) Mesh of the model. c) Boundary conditions (bc) and loading of the sample to model all phases of the triaxial test in different variations, e.g. pressure or volume controlled loading and drained or undrained conditions at the end plates.

To analyse the stress state around the filter tip at the moment the fracture occurs, the simulations were evaluated at the corresponding point of time t_{fr} at which the fracturing pressure was reached in the laboratory test variation.

3.2 Critical stress states

In the numerical calculations no failure criteria were given as the fracture criteria for fine-grained soil is unknown. But by using the MCC model the critical state line (CSL) is included. Fractures can be triggered by tensile and or shear stresses, hence in the postprocessing both were analysed at the moment of fracture initiation t_{fr}. The numerical analysis of the tests on consolidated samples show, that at $t = t_{fr}$ an area around the filter tip exists in which the minor principal stress σ_{min} becomes tensile stress or in which the shear stress ratio $\eta = q/p$ with the deviator stress q reaches the CSL. In the following these areas are called critical stress zones. The size of these zones as well as the maximum tensile or shear stress intensity within the zone correlate primarily with the sample's material and the overconsolidation ratio. In other words, the stress analysis of test variations with the same material and OCR show almost identical critical stress zones independent from the drainage condition, the backpressure and the v/k -ratio. Even the initial stress state has in fact little influence on these critical areas. This is demonstrated in Figure 4 by field plots of the stress ratio η at $t = t_{fr}$ for the test series on silt with different initial mean stresses of $p =$ 100 kPa, 200 kPa and 300 kPa. The critical zones in which the stress ratio reaches the CSL of silt with $\eta \geq M_c = 1{,}4$ is displayed in grey. The size of the grey zone grows only slightly with p. In contrast Figure 5 shows the field plots of the test series on silt with $OCR = 1, 2$ and 4.

The grey zones of the c critical shear stress with $\eta \geq 1{,}4$ and of tensile stress $\sigma_{min} \leq 0$ kPa grow with the increase of OCR.

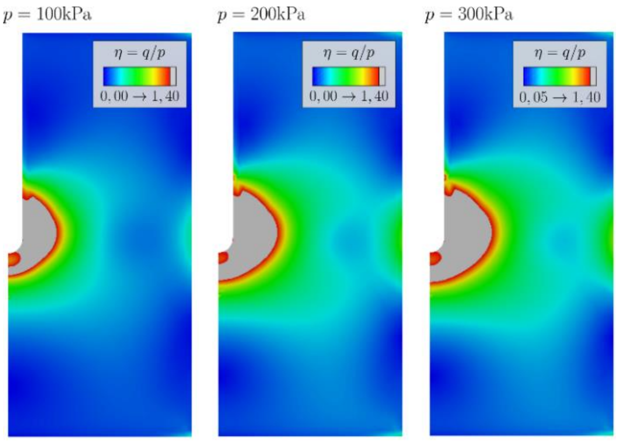

Figure 4. Stress ratio η at the moment of fracturing for test variations with different initial mean stresses p. The grey zone where the maximum stress ratio of $M_c = 1{,}4$ is reached increases only slightly with p.

The conclusion from this numerical analysis was drawn with a view on the basics of fracture mechanics.

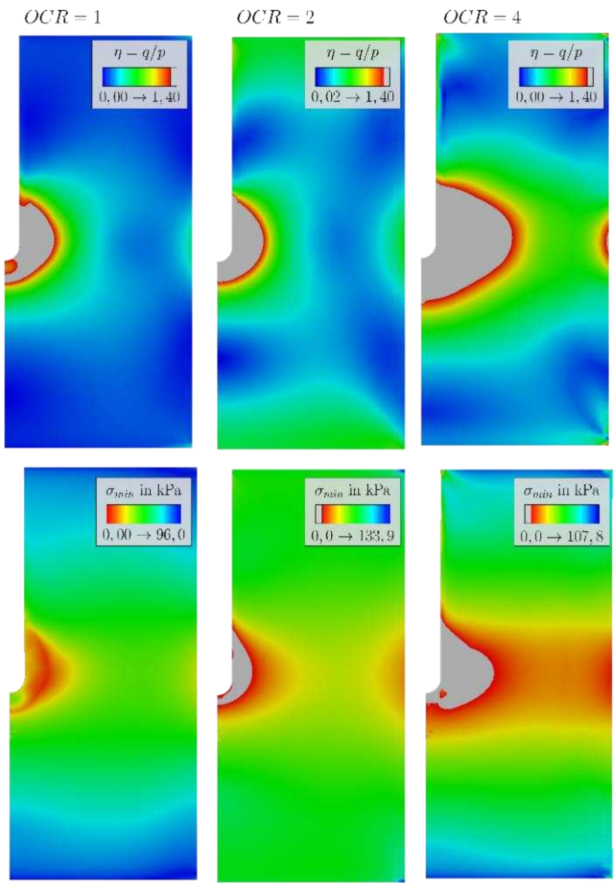

Figure 5. Stress ratio η (upper row) and minimum principal stress σ_{min} (lower row) at the moment of fracturing for test variations with different overconsolidation ratios OCR. The grey zone where the maximum stress ratio of $M_c = 1{,}4$ is reached or the σ_{min} is tensile increases with OCR.

According to these fractures initiate at an imperfection in the material, where high tensile or shear stress loads occur. If these stress intensities at an imperfection reach the materials specific critical value, the fracture extends from the imperfection. If the pore structure of a homogenous material in which larger pores, extraneous inclusions or little fissures represent imperfections, then the fracture initiates if in the critical stress zone around the filter tip the material strength is reached at one of these imperfections.

This results in a probabilistic issue: as the pore water pressure at the filter tip increases, the critical stress zone grows and with it the probability that there is an imperfection in this area where the material strength is exceeded. If this zone varies in its size when fracture occur, the material will either differ in strength or in the amount and size of imperfections.

4 CONCLUSIONS

With the newly developed triaxial test for hydraulic induced fractures in soil reproducible results regarding the fracturing pressure in consolidated fine-grained samples can be obtained. In an extensive laboratory study the material of the samples, the initial stress state, the overconsolidation ratio and the rate of the hydraulic loading were identified as the decisive factors influencing the fracturing pressure. A numerical analysis of the stress state at the time of fracture initiation in the test variations of the study show that there are similar zones of high tensile or shear stress around the filter tip. The size of this zone and the level of tension or shear depends only on the material, the overconsolidation ratio and slightly on the initial stress state.

Based on this numerical analysis and the fundamentals of fracture mechanics, it can be hypothesised that the hydraulically induced fractures in the samples are only influenced by three factors: the material resistance, the effective stress state and the defects in the material.

REFERENCES

Eurocode 7 – Geotechnical design – Part1: General rules; German version EN 1997-1:2004+AC:2009+A1:2013. 2014. Beuth.

Günther, H. (2019) Development of a triaxial test for hydraulic loading of fine-grained soil. In *Proceedings of the XVII ECSMGE-2019 Geotechnical Engineering foundation of the future,* Reykjavik, Iceland. https://doi.org/10.32075/17ECSMGE-2019-0055.

Machacek, H. (2024) *Analyse von Einflussfaktoren des Widerstands feinkörniger Böden bei hydraulischer Belastung*. Phd-Thesis Bauhaus Universität Weimar.

Machacek, H. and Odenwald, B. (2023). Nachweise bei umströmten Wänden in bindigen Böden – Ansätze und experimentelle Untersuchungen, In: *Kolloquium Geohydraulische Aspekte bei Baumaßnahmen des Verkehrswasserbaus,* Karlsruhe, Germany, pp. 69-79.

Jaworski, G.W., Seed, H.B. and Duncan, J. M. (1981) Laboratory study of hydraulic fracturing. *Journal of the Geotechnical Engineering Division,* 107(6), pp. 713-732, https://doi.org/10.1061/AJGEB6.0001147.

Wudtke, R.-B. (2014) *Hydraulischer Grundbruch in bindigem Baugrund*. Phd-Thesis Bauhaus Universität Weimar.